Orbital-angular-momentum crosstalk and temporal fading in a terrestrial laser link using single-mode fiber coupling

Gustavo Funes,[1] **Matías Vial,**[1] **and Jaime A. Anguita**[1,2,*]

[1]*Facultad de Ingeniería y Ciencias Aplicadas, Universidad de los Andes Mons. Alvaro del Portillo 12455, Las Condes, 7620001 Santiago, Chile*

[2]*Center for Optics and Photonics, Universidad de Concepción, Casilla 4012, Concepción, Chile*

[*] *janguita@miuandes.cl*

Abstract: Using a mobile experimental testbed, we perform a series of measurements on the detection of laser beams carrying orbital angular momentum (OAM) to evaluate turbulent channel distortions and crosstalk among receive states in an 84-m roofed optical link. We find that a receiver assembly using single-mode fiber coupling serves as a good signal selector in terms of crosstalk rejection. From the recorded temporal channel waveforms, we estimate average crosstalk profiles and propose an appropriate probability density function for the fluctuations of the detected OAM signal. Further measurements of OAM crosstalk are described for a horizontal 400-m link established over our campus.

OCIS codes: (060.4510) Optical communications; (080.4865) Optical vortices; (010.1300) Atmospheric propagation.

References and links

1. S. Arnon, "Effects of atmospheric turbulence and building sway on optical wireless-communication systems," Opt. Lett. **28**, 129–131 (2003).
2. G. Gibson, J. Courtial, and M. Padgett, "Free-space information transfer using light beams carrying orbital angular momentum," Opt. Express **12**, 5448–5456 (2004).
3. M. Dennis, K. O'Holleran, and M. Padgett, "Singular optics: optical vortices and polarization singularities," Prog. Optics **53**, 293–363 (2009).
4. G. Berkhout, M. Lavery, J Courtial, M. Beijersbergen, and M. Padgett, "Efficient Sorting of Orbital Angular Momentum States of Light," Phys. Rev. Lett. **105**, 153601 (2010).
5. S. Li and J. Wang, "Performance evaluation of analog signal transmission in an orbital angular momentum multiplexing system," Opt. Lett. **40**, 760–763 (2015).
6. I. B. Djordjevic, J. A. Anguita, B. Vasic, "Error-correction coded orbital-angular-momentum modulation for FSO channels affected by turbulence," J. Lightwave Technol. **30**, 2846–2852 (2012).
7. J. A. Anguita, J. Herreros, I. B. Djordjevic, "Coherent multimode OAM superpositions for multidimensional modulation," IEEE Photon. J. **6**, 1–11 (2014).
8. J. Wang, J.-Y. Yang, I. M Fazal, N. Ahmed, Y. Yan, H. Huang, Y. Ren, Y. Yue, S. Dolinar, M. Tur, and A. E. Willner, "Terabit free-space data transmission employing orbital angular momentum multiplexing," Nature Photon. **6**, 488–496 (2012).
9. J. A. Anguita, M. Neifeld, and B. Vasic, "Turbulence-induced channel crosstalk in an orbital angular momentum-multiplexed free-space optical link," Appl. Opt. **47**, 2414–2429 (2008).
10. M. Malik, M. O'Sullivan, B. Rodenburg, M. Mirhosseini, J. Leach, M. P. J. Lavery, M. J. Padgett, and R. W. Boyd, "Influence of atmospheric turbulence on optical communications using orbital angular momentum for encoding," Opt. Express **20**, 13195–13200 (2012).

#243775 Received 25 Jun 2015; revised 12 Aug 2015; accepted 13 Aug 2015; published 25 Aug 2015

11. Y. Ren, H. Huang, G. Xie, N. Ahmed, Y. Yan, B. I. Erkmen, N. Chandrasekaran, M. P. J. Lavery, N. K. Steinhoff, M. Tur, S. Dolinar, M. A. Neifeld, M. J. Padgett, R. W. Boyd, J. H. Shapiro, and A. E. Willner, "Atmospheric turbulence effects on the performance of a free space optical link employing orbital angular momentum multiplexing," Opt. Lett. **38**, 4062–4065 (2013).
12. G. Tyler and R. Boyd, "Influence of atmospheric turbulence on the propagation of quantum states of light carrying orbital angular momentum," Opt. Lett. **34**, 142–144 (2009).
13. B. Rodenburg, M. Lavery, M. Malik, M. O'Sullivan, M. Mirhosseini, D. J. Robertson, M. Padgett, and R. W. Boyd, "Influence of atmospheric turbulence on states of light carrying orbital angular momentum," Opt. Lett. **37**(17), 3735–3737 (2012).
14. H. Huang, Y. Cao, G. Xie, Y. Ren, Y. Yan, C. Bao, N. Ahmed, M. A. Neifeld, S. J. Dolinar, and A. E. Willner, "Crosstalk mitigation in a free-space orbital angular momentum multiplexed communication link using 4×4 MIMO equalization," Opt. Lett. **39**, 4360–4363 (2014).
15. Y. Ren, G. Xie, H. Huang, C. Bao, Y. Yan, N. Ahmed, M. P. J. Lavery, B. I. Erkmen, S. Dolinar, M. Tur, M. A. Neifeld, M. J. Padgett, R. W. Boyd, J. H. Shapiro, and A. E. Willner, "Adaptive optics compensation of multiple orbital angular momentum beams propagating through emulated atmospheric turbulence," Opt. Lett. **39**, 2845–2848 (2014).
16. P. Bierdz, M. Kwon, C. Roncaioli, and H. Deng, "High fidelity detection of the orbital angular momentum of light by time mapping," New J. Phys. **15**, 113062 (2013).
17. H. Qassim, F. M. Miatto, J. P. Torres, M. J. Padgett, E. Karimi, and R. W. Boyd, "Limitations to the determination of a Laguerre-Gauss spectrum via projective, phase-flattening measurement," J. Opt. Soc. Am. B **31**, A20–A23 (2014).
18. J. A. Anguita and J. Herreros, "Experimental analysis of orbital angular momentum-carrying beams in turbulence," Proc. SPIE **8162**, 816207 (2011).
19. L. Andrews, R. Phillips, *Laser Beam Propagation through Random Media* (SPIE Press, 1998).
20. S. Kotz and J. R. van Dorp, *Beyond Beta: Other Continuous Families of Distributions with Bounded Support and Applications* (World Scientific Publishing Company, 2004).

1. Introduction

Laser communications over unguided channels open new possibilities for point-to-point satellite and/or terrestrial links and access networks. In terrestrial laser communications, the effects of atmospheric turbulence must be properly acknowledged, and communication channels should be well modeled in order to design robust links under operational cost constraints [1, 2]. Laser communications may improve in bandwidth and robustness with the use of specialty beams carrying orbital angular momentum (OAM). OAM-carrying laser modes rotate around their propagation axis and feature a dark central spot due to their phase dislocation. A collection of coaxial modes with distinct integer OAM states form an orthogonal set of functions [3]. Consequently, an optical system can superimpose and afterwards separate constituent modes without interference [4]. Such property allows the use of OAM modes for space division multiplexing (SDM) communication channels and/or for multi-dimensional modulation of the carriers [5–7]. Communication using simultaneous OAM channels has been tested in ideal conditions showing promising results [8].

Recent works have also shown that OAM modes are disturbed as they propagate through the turbulent atmosphere, in which spatial variations of the refractive index of the air modify the phase structure of the vortex. In such case, single-state OAM signals are spread over several states, thus, impairing the detection and increasing symbol-error rate [9–11]. Therefore, the received signal carried on a particular OAM mode may actually include the signal leaked from other channels resulting in a poor system performance. This effect is usually called crosstalk and has been studied over the last years using numerical propagation models or by experimentation using screen-based synthetic turbulence. See the work in [9–13] and references therein. Moreover, some successful systems have been proposed for crosstalk mitigation like MIMO [14] and adaptive optics [15].

Most of the previous studies of OAM crosstalk and signal fluctuations utilize numerical simulations or back-to-back experimental setups where the turbulence volume or the "atmosphere" is represented by thin-phase screens. Such approach is widely used in astronomy, where the

#243775 Received 25 Jun 2015; revised 12 Aug 2015; accepted 13 Aug 2015; published 25 Aug 2015

influence of turbulence is relevant in a thin region near the observer. However, in the case of slant-angle and horizontal point-to-point terrestrial communication links, turbulence has to be integrated over the path. For this reason, thin-phase models may be insufficient to represent temporal intensity fluctuations of OAM-bearing signals and crosstalk.

In this paper we test a transmit/receive optical setup to evaluate the OAM detection and crosstalk temporal fluctuations around each transmit state over an 84-m horizontal link that is subject to weak turbulence. Detection of OAM signals is accomplished by single-mode-fiber coupling after vortex phase cancellation, in contrast to spatial filtering based on pinholes [16–18]. Probability densities are matched to the histograms of the recorded temporal sequences, showing a good and systematic fit. An extension of this experiment is performed outdoors, in a 400-m link under intermediate-to-strong turbulence.

2. System description

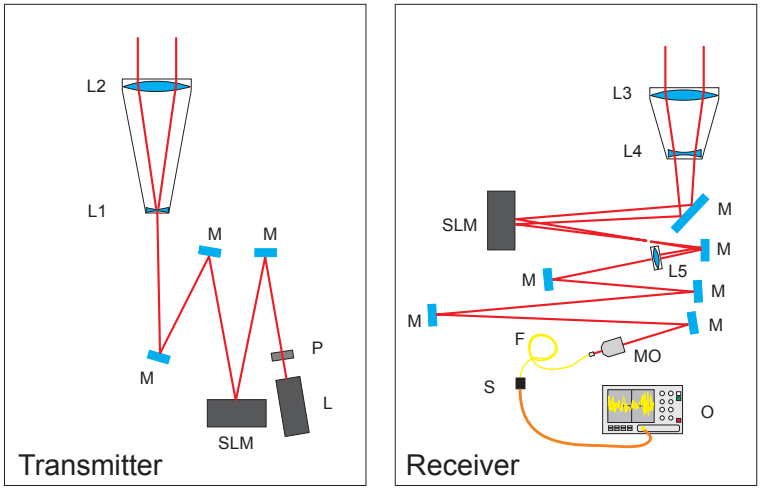

Fig. 1. Experimental schematic for the 84 m link placed under a roofed hallway. The link is completed using a flat, 4” mirror placed about 42 m away from the transmit/receive assembly.

To test the principle of vortex rejection in a single-mode fiber, a back-to-back evaluation was performed. The test comprised a linearly-polarized zero-order Gaussian beam directed onto a spatial-light modulator (SLM, Holoeye Pluto NIR) programmed with a forked blazed grating with a given OAM state (see [7] for details). The first diffracted order containing a Laguerre-Gauss (LG) beam —or more precisely, a superposition of radial LG modes with the same OAM state— is directed towards the second SLM, 1.5 m apart from the first, in which the reversed helical OAM phase structure has been programmed (i.e., the analyzing grating). The diffracted field emerging from the analyzing grating is a vortex-free ring —which we call vortex cancellation— that is passed through two converging lenses in order to obtain an enlarged far-field distribution [2]. The resulting field —separated from the unwanted residual diffracted light— is coupled into the single-mode fiber by means of a microscope objetive lens assembly mounted on a tridimensional stage. By changing the OAM state in the analyzing grating, it is possible to measure the power leaked to the adjacent states. To check for reliability, states -10 to +10 were tested. The measured optical extinction ratio was below -13 dB on immediately adjacent states and less than -22 dB two states apart. These results are as good as those seen when a pinhole-detector combination is used [18]. With this preliminary test

#243775 Received 25 Jun 2015; revised 12 Aug 2015; accepted 13 Aug 2015; published 25 Aug 2015

it can be concluded that single-mode fiber coupling is able to filter out optical vortices with great efficiency in the absence of atmospheric perturbations. Note that poor fiber alignment may lead to larger crosstalk power.

The main experiment consisted on the generation, expansion and propagation of a range of OAM states along a covered hallway that is open on both sides, but is not directly exposed to sunlight or strong winds. This quasi-outdoor path serves well as a test for the system stability in a situation where the propagation is comparable to short building-to-building links, but the turbulence is weak. As shown in Fig. 1, the transmitter comprises a 40 mW laser diode with wavelength 660 nm that is collimated using an aspherical lens to produce a 5 mm beam. The beam passes through a linear polarizer (P), it is reflected on a mirror (M) and aimed to an SLM with a small angle of incidence. The emerging OAM beam is reflected by two mirrors (M) and directed into an $7\times$ expanding telescope. The latter was adjusted to produce a beam waist at 42m (half way). This ensures that the beam has approximately the same diameter at both the emitter and the receiver. At the receiver end, the beam is collected by a compressing telescope. The vortex is aligned to the analyzing SLM, whose first diffraction order passes through a converging lens (L5). Finally, the analyzed beam is collected by a microscope objective (MO), coupled into a SM600 single-mode fiber (F) and detected with a photodiode sensor (S). The electric signal is recorded in a digital oscilloscope (O).

A 4-inch flat mirror ($\lambda/10$) is mounted on a platform located at the end of the hallway to complete the optical path that extends to approximately 84 m. A wireless remote-control system was developed to adjust the mirror mount in order to redirect the beam onto the receiver ($20\,\mu$rad resolution). Blazed forked gratings were used in all cases, as described in [7]. An effort was put in reducing the intensity losses at the transmission SLM by means of good adjustment of polarization and reduction of aberrations. This ensures a correct distribution of energy over all diffraction orders and good ring formation. With the described configuration it is possible to couple up to 20% of the optical power incident at the receive telescope. Figure 2 depicts images of OAM beams produced with the described setup, with states 4 to 50, obtained at the exit of the transmit telescope.

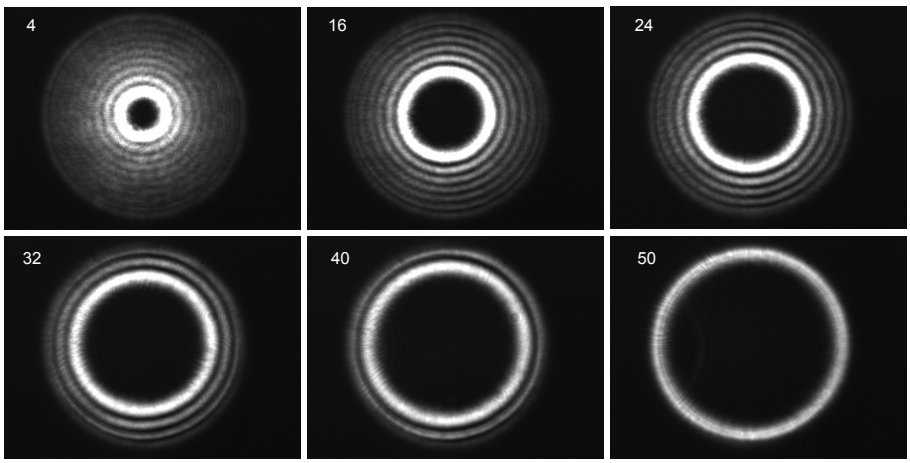

Fig. 2. Sample experimental OAM beams photographed at the exit of the expanding telescope. From top left, states 4, 16, 24, 32, 40, and 50.

#243775 Received 25 Jun 2015; revised 12 Aug 2015; accepted 13 Aug 2015; published 25 Aug 2015

3. OAM crosstalk measurements

In order to understand OAM signal fluctuations and establish a statistical model, we planned a systematic experiment to record the received optical waveforms using a low-noise detector and a oscilloscope. The procedure to obtain significant statistics is as follows. Using the experimental setup described above, LG modes with states 0 to 10 were transmitted and detected one at a time. Transmit optical power was set high enough to produce a large signal-to-noise ratio at the oscilloscope, thus, allowing the detection of weak crosstalk events away from the noise floor. The analyzing SLM was set to scan seven states around the transmitted OAM state, three at each side. Time waveforms spanning 20 seconds, sampled at 5 kHz, were recorded for each combination of transmit-receive OAM state. Because real atmospheric variations do not behave as an stationary random process, ocasional spurious falloffs and changes in amplitud along the recorded waveforms were discarded and immediately remade (*in situ*) to avoid misleading statistical results [19].

A practical representation of received signal fluctuations is through a histogram. In Fig. 3, two sets of histograms of received signals are plotted. The first row corresponds to signal detection on OAM states -1, 0, 1, 2, and 3 when OAM state 1 has been transmitted. Thus, the central histogram corresponds to the power remaining on the intended state (cancelled vorticity), while the other histograms in (a) correspond to the crosstalk. The received optical power has been normalized by the maximum signal on the intended state, to favor an easy side-by-side comparison. In weak turbulence conditions —quantified with more detail in Section 6— the power remaining on the intended state is concentrated closer to a value of 1. In contrast, histograms of crosstalk show values near 0. On Fig. 3(b), the signal has been measured on states 5, 6, 7, 8, and 9 when OAM state 7 has been transmitted. In this example, a stronger turbulence produces larger spreading on the intended state, while crosstalk behaves similarly as before, although with a larger spreading.

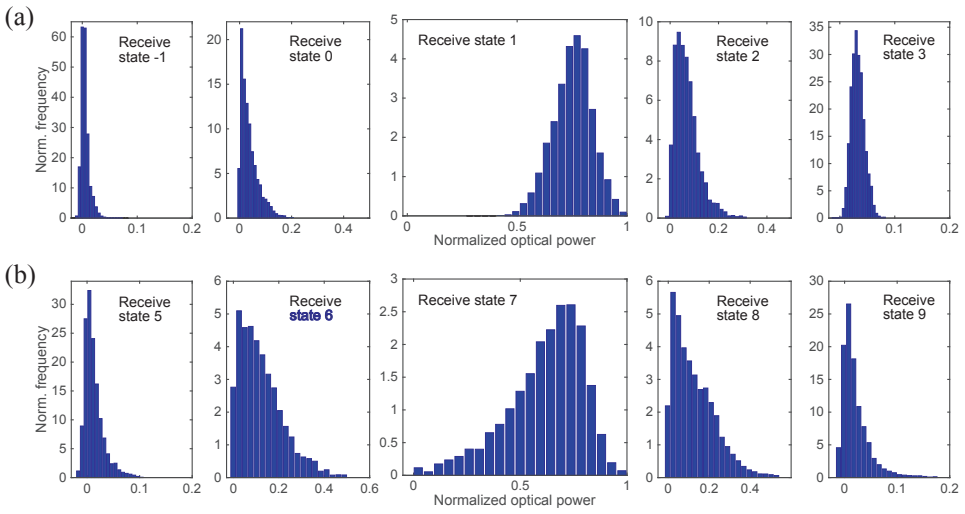

Fig. 3. Histograms of the received optical signal. (a) For transmit OAM state 1. (b) For transmit state 7.

These histograms make apparent that random signal fading after OAM detection does not distribute as the fading from typical free-space laser links based on zero-order Gaussian beams do. By comparing the two rows of histograms one can infer that the larger the spreading of the

#243775 Received 25 Jun 2015; revised 12 Aug 2015; accepted 13 Aug 2015; published 25 Aug 2015

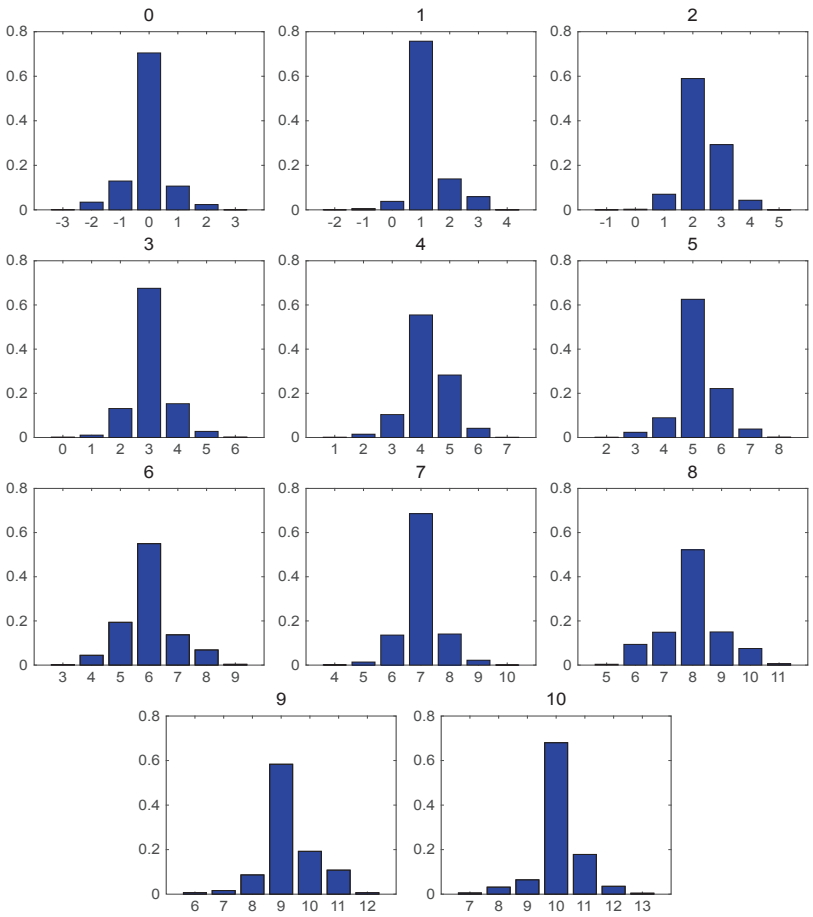

Fig. 4. Time-average received signals and crosstalk on adjacent states for OAM states 0 to 10 (indicated on top of each plot). Bars in each plot have been normalized by the total received optical power. Signals recorded with the 84-m experiment.

intended state's histogram, the larger will be crosstalk histogram spreading. These examples are representative of all histograms obtained within the studied range.

The average intended signal and average crosstalk for states 0 to 10 are shown in Fig. 4, exhibiting a good correspondence to previous numerical simulations [9]. We observe an overall symmetry in average crosstalk around the intended state. Larger crosstalk bars occur randomly on either side, but are not systematic. We leave them as measured, to show realistic experimental outcomes subject to the described procedure. Although higher state numbers could be tested, we limited this part of the study to the aforementioned range to ensure a relatively short data acquisition process. Since beam wander and scintillation affect the angle of arrival and the wavefront coherence, respectively, these phenomena could be responsible for temporarily misaligning the optical setup and undermining the vortex cancellation.

Also of interest, the crosstalk for some cases happen to be near 50% of the energy remaining on the state of interest. This seems to occur in a randomly fashion, and does not appears to depend on the transmission state, at least within the tested range. Again, we argue that real atmospheric turbulence causes important disruptive effects from time to time. Long-term turbu-

#243775 Received 25 Jun 2015; revised 12 Aug 2015; accepted 13 Aug 2015; published 25 Aug 2015

lence fluctuations may influence entire measurement runs. For this reason, this experiment was repeated and similar results were obtained, supporting the validity of our hypothesis. The Rytov variance was $\sigma_R^2 < 0.01$ for all these cases, although C_n^2 was in the intermediate turbulence regime, at it is shown in Section 6.

4. Outdoor propagation experiment

The second experiment consisted on the propagation of vortices along a horizontal 400m path. In this case the transmitter/receiver assembly was placed on an open balcony (at the Main Library) and the flat mirror was placed at the far end of another building's roof, 200 m away, at approximately 15 m above the ground. A few terraces, walls, and a road that accumulate heat during the day are found along the propagation path. All experiments in this range were performed after sunset, to reduce technical difficulties. Most of them were taken from 18:00 hrs to 22:00 hrs. Since this is a true outdoor propagation range, we were able to observe all transient events occurring in atmospheric turbulence. Particularly, beam wander was much stronger than the that observed in the 84-m link. Beam distortions due to small turbulence cells further affected measurements, by reducing the beam wavefront coherence and, thus, enlarging the point spread function.

The experimental setup was similar to the setup described in the Section 2. A larger receive telescope (8-inch Schmidt-Cassegrain, with a 2-inch central obstruction) was used in this case. In order to propagate higher order OAM beams, the waist of the transmit beam was modified and estimated to be at about 100 m from the transmitter, but could not be determined with precision due to the height of the beam and the increased turbulence.

In this scenario, the OAM states transmitted ranged from 22 to 36 to accommodate the telescope's central obstruction. The vortex cancellation was performed using gratings with states 0 to 50 (even numbers). The crosstalk histograms for a few detected OAM states are shown in Fig. 5. It can be seen that a high amount of energy was leaked to the adjacent states and for some modes the bar representing the intended OAM cancellation is not the tallest. We have marked the intended state with a red arrow in each plot. We could not determine wether the average crosstalk was symmetric, with the exception of a few cases, as scintillation reached values above 1.0 in many occasions.

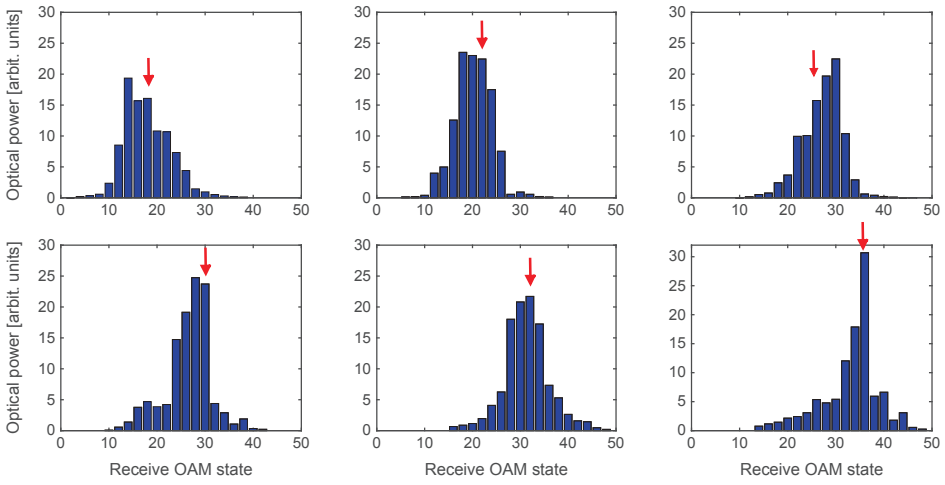

Fig. 5. Experimental OAM transmission over 400 m. Time average signal measured at receive OAM states 0 to 50. Transmited states are marked with an arrow within each plot.

#243775 Received 25 Jun 2015; revised 12 Aug 2015; accepted 13 Aug 2015; published 25 Aug 2015

In spite of the preliminar results in Fig. 5, detection of signals on distinct OAM states should be still feasible if the distance between state is large enough for a given turbulence strength. As described later on in Section 6, turbulence is strong in this setup, allowing a larger leakage on adjacent states. However, it appears to be constrained within 8 states on each side of the cancelled vortex. Also, we note that histograms in Fig. 5 do not resemble those obtained by simulations, and further experimentation is required.

5. Probability models for OAM signal fluctuations

For signals on intended states we have fitted a Johnson S_B probability density function (PDF). The Johnson S_B PDF is part of a family of distributions and is derived from a transformation of a Normal PDF [20]. If a random variable X is Normally distributed (with parameters $\{0,1\}$), a random variable Y in the relation $X = \gamma + \delta g(Y)$, or equivalently $Y = g^{-1}\left(\frac{X-\gamma}{\delta}\right)$, will distribute according to a Johnson S_B probability function if $g(y) = \ln[y/(1-y)]$. The Johnson S_B PDF is given by

$$f_Y(y|\gamma,\delta) = \frac{\delta}{\sqrt{2\pi}} \frac{1}{y(1-y)} \exp\left\{-\frac{1}{2}\left[\gamma + \delta \log\left(\frac{y}{1-y}\right)\right]^2\right\} \tag{1}$$

where γ and δ are the parameters of the distribution. Now, since $0 \leq y \leq 1$ the cumulative distribution presented above is not available in a closed form. Two additional parameters are introduced, μ and σ that control the function domain through the transformation $z = \sigma y + (\mu + \sigma)$ and μ is the bias or location parameter, while σ is the scale parameter. The latter two act together as $\mu < z < \mu + \sigma$.

Using the transformation given above and considering that X is Normal, parameters γ and δ can be quickly estimated. We have found that for all OAM channels, the Johnson S_B PDF approximates the histograms with a coefficient of determination (R^2) from 0.93 to 0.99 approximately. This distribution appears to fit well with the experimental data obtained in the 84m path, as can be seen on the left column of Fig. 6. In spite of the stronger atmospheric fluctuations, for the 400-m data series we have also found a good correspondence with the Johnson S_B distribution. These results can be seen in the right column of Fig. 6. By comparing left and right columns of Fig. 6, it is clear that the 400-m data series have a tendency towards zero intensity. This means that the signal have considerable power losses, whereas the cancellation signals for the 84 m experiment are hardly near zero. A long path makes alignment challenging and due to the unsteadiness of weather conditions, measurements were not uniformly affected. The parameters of the PDFs are given in the plots.

6. Turbulence strength estimation

Turbulence is one of the main effects that disrupts the vortex propagation in the channel. Not only the refractive index fluctuations have a strong influence but also the propagation distance acts as a multiplier for these effects. That is why turbulence strength needs to be estimated for each experimental channel.

Measuring C_n^2 comes straightforward from the variance of beam wandering assuming the outer scale is infinite [19]. This variance is given by

$$\langle r^2 \rangle = 2.42 C_n^2 L^3 W_0^{-1/3} {}_2F_1(1/3, 1; 4; 1 - |\Theta_0|), \tag{2}$$

where Θ_0 can be obtained from the focal plane, and W_0 is the beam radius at the emitter.

Turbulence strength was evaluated using a separate measurement since this model requires a Gaussian beam instead of a vortex. The beam focus is estimated to be approximately at 100 m for the 400-m experiment and at 42 m for the indoor one. The variance of wandering is obtained

#243775 Received 25 Jun 2015; revised 12 Aug 2015; accepted 13 Aug 2015; published 25 Aug 2015

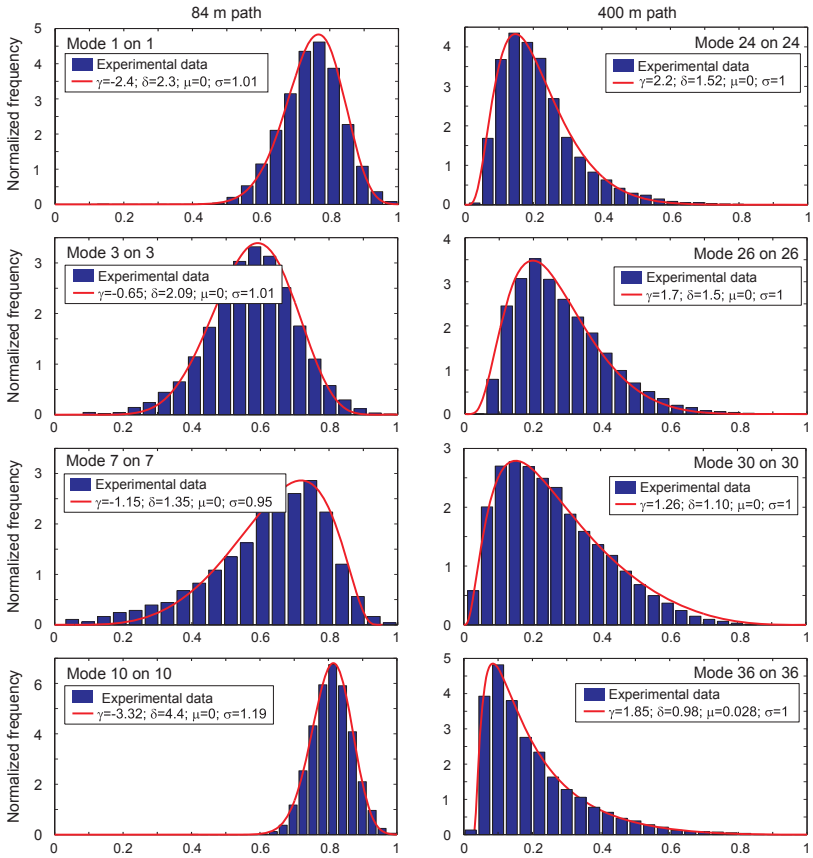

Fig. 6. Histogram representation for some detected OAM signals and the fit of a JohnsonS_B probabilty density function. Left column: 84-m range. Right column: 400-m range.

through the displacement of the beam's centroid registered on a CCD camera. Measurements at both ranges took three hours, recording 800 images at a rate of 200 Hz, every ten minutes. The results are shown in Fig. 7. As expected, turbulence strength has a tendency of decay at night, varying from 10^{-13} to roughly 5×10^{-15}. Since both experiments have been performed at different paths, knowing C_n^2 only is insufficient to discern from weak to strong turbulence. For that reason we have calculated the Rytov variance and added it to the figure. In this case it can be seen that the short range is exposed to weak turbulence whereas the long range shows a peak in $\sigma_R^2 = 1.09$ that can be considered strong turbulence. As the time passes, it decays to 0.06. Nevertheless, even the smallest scintillation value is still nearly one order of magnitude higher than that of the short range.

7. Conclusion

The propagation and detection of Laguerre-Gauss beams with different OAM states is demonstrated in outdoor ranges to determine the OAM crosstalk —i.e., the spreading of energy from an intended OAM state to other non-intended states— induced by true atmospheric turbulence. In the short range —84 m in a roofed open hallway—, we could verify the relationship between crosstalk and turbulence strength (although only qualitatively at this time) and the particular scintillation behavior exhibited by the detected OAM state. We find that temporal fluctuations

#243775 Received 25 Jun 2015; revised 12 Aug 2015; accepted 13 Aug 2015; published 25 Aug 2015

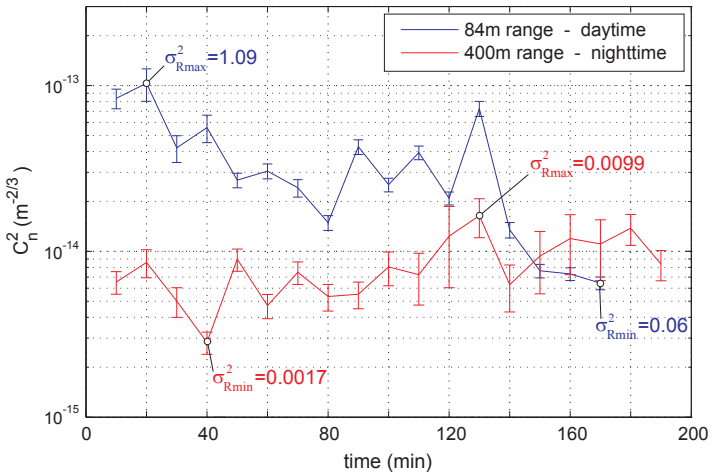

Fig. 7. Turbulence strength estimation for the short range (red) and long range (blue) experiments. The long-range data was recorded from 18:05 hrs to 21:00 hrs, while the short-range data was recorded from 13:20 hrs to 16:20 hrs.

of any detected OAM state can be well modeled by the Johnson-S_B probability density function, which can differ significantly from the Lognormal or Gamma-Gamma densities, particularly in weak turbulence conditions. Further experimental tests are performed over a 400m range showing that in strong turbulence scenarios, the power remaining on the transmit state may in some cases be lower than that on the crosstalk. Temporal distribution in those high-scintillation events may still be modeled by the Johnson-S_B distribution.

Acknowledgments

This work has been funded in part by CONICYT under grant FR-1120971 and by PIA-CONICYT PFB0824.

#243775 Received 25 Jun 2015; revised 12 Aug 2015; accepted 13 Aug 2015; published 25 Aug 2015